Quadruple Bonds between Molybdenum Atoms Supported by Alkoxide Ligands

Malcolm H. Chisholm,* Kirsten Folting, John C. Huffman, Elena F. Putilina, William E. Streib, and Robert J. Tatz

Department of Chemistry and Molecular Structure Center, Indiana University, Bloomington, Indiana 47405

Received February 11, 1993

The reaction between $Mo_2(i\text{-}Bu)_2(NMe_2)_4$ and excess 2-propanol in hexane yields the mixed alkoxide/alcoholate $Mo_2(O\text{-}i\text{-}Pr)_4(HO\text{-}i\text{-}Pr)_4$ (**1**) by way of amide for alkoxide exchange (alcoholysis) and reductive elimination of isobutane and isobutylene. A similar reaction involving cyclopentanol gives $Mo_2(O\text{-}c\text{-}Pen)_4(HO\text{-}c\text{-}Pen)_4$ (**2**). The reaction between $Mo_2(i\text{-}Bu)_2(NMe_2)_4$ and 4 equiv of neopentanol in hexane yields the dimethylamine adduct $Mo_2(OCH_2\text{-}t\text{-}Bu)_4(HNMe_2)_4$ (**3**). Compounds **1–3** have been crystallographically characterized, and in each compound there is a Mo–Mo quadruple bond supported by four alkoxide ligands and four ligands (ROH or Me_2NH) that form hydrogen bonds to the alkoxide ligands. The Mo–Mo distances fall in the range 2.11–2.13 Å, typical of those seen in Mo–Mo quadruply bonded complexes. These compounds are substitutionally labile, and $Mo_2(O\text{-}i\text{-}Pr)_4(HO\text{-}i\text{-}Pr)_4$ (**1**) reacts with pyridine in hydrocarbon solvents to give $Mo_2(O\text{-}i\text{-}Pr)_4(py)_4$ (**4**), and the dimethylamine adduct, **3**, reacts similarly with PMe_3 to give $Mo_2(OCH_2\text{-}t\text{-}Bu)_4(PMe_3)_4$ (**5**). Compounds **4** and **5** have also been structurally characterized and are found to have unusually long Mo–Mo distances, 2.195(1) Å for **4** and 2.218(2) Å for **5**. The Mo–OR distances are all long relative to $Mo_2(OR)_6$ and $Mo_2(OR)_6L_2$ compounds (L = py, PMe_3, etc.) and show a consistent pattern. For compounds **4** and **5**, the Mo–OR distances are 2.03 and 2.04 Å (average), respectively, while in the presence of the hydrogen-bridged compounds **1–3**, the Mo–OR distances are notably longer, 2.08–2.13 Å. In the mixed alkoxide/alcoholate compounds, it is not possible to uniquely distinguish between Mo–OR and Mo–O(H)R bonds. Indeed, on the basis of the chemical shift values for the OH---O and OD---O protio and deuterio complexes, respectively, we observe a negative $\Delta\delta(^1H,^2H)$ value which is indicative of a symmetrical hydrogen bond. This contrasts with other mixed alkoxide/alcoholate complexes such as $M_2(O\text{-}i\text{-}Pr)_8(HO\text{-}i\text{-}Pr)_2$, which have unsymmetrical hydrogen bridges and rather different M–O distances to the M–OR and M–O(H)R groups (M = Zr, Ce). The long Mo–O distances, the relatively small Mo–O–C angles, typically less than 130°, and the long Mo–Mo quadruple-bond distances in **4** and **5** reflect the mutually unfavorable filled–filled O p_π–Mo d_π interactions. The presence of the hydrogen atom bridges in compounds **1–3** serves to decrease this effect. The compounds have also been characterized by UV–visible, NMR, and IR spectroscopy. The substitutional lability of compound **1** has been investigated by following the kinetics of protio 2-propoxide/2-propanol ligand exchange with $i\text{-Pr-}d_7\text{-OD}$ (100-fold excess) at low temperatures by ^1H NMR spectroscopy. Under these conditions the substitution obeyed pseudo-first-order kinetics and yielded the activation parameters $\Delta H^\ddagger = 9.5(5)$ kcal mol^{-1} and $\Delta S^\ddagger = -34(3)$ eu, which are consistent with an associative reaction mechanism. Summary of crystal data: for **1** at −170 °C, a = 12.810(4) Å, b = 12.810(4) Å, c = 9.896(5) Å, $Z = 2$, d_{calcd} = 1.37 g cm^{-3}, space group $P4/mnn$; for **2** at −164 °C, a = 62.232(11) Å, b = 10.442(2) Å, c = 20.167(3) Å, β = 106.83(1)°, $Z = 12$, d_{calcd} = 1.39 g cm^{-3}, space group $C2/c$; for **3** at −160 °C, a = 22.064(5) Å, b = 22.064(5) Å, c = 16.985(4) Å, $Z = 8$, d_{calcd} = 1.16 g cm^{-3}, space group $I4cm$; for **4** at −167 °C, a = 18.254(6) Å, b = 10.327(20 Å, c = 10.076(2) Å, α = 70.92(1)°, β = 103.08(1)°, γ = 104.38(1)°, $Z = 2$, d_{calcd} = 1.44 g cm^{-3}, space group $P\bar{1}$; for **5** at −162 °C, a = 19.441(10) Å, b = 11.619(5) Å, c = 9.906(4) Å, β = 106.41(2)°, $Z = 2$, d_{calcd} = 1.31 g cm^{-3}, space group Pa.

Introduction

The so-called d^3–d^3 dimers of molybdenum and tungsten display a rich coordination chemistry,[1,2] and the ethane-like dimers of formula M_2X_6 where X = alkyl,[3] amide,[4,5] alkoxide,[6,7] thiolate,[8] selenolate,[9] etc. hold a pivotal position. In previous studies of the mixed alkyl/amido compounds of formula $M_2R_2(NMe_2)_4$, some rather interesting phenomena were discovered in their reactions with alcohols.[10] First, kinetically the amido groups were replaced in preference to the alkyl ligands despite the known bond strengths D(M–O) > D(M–N) > D(M–C). Second, in the case of M = Mo and R = a β-hydrogen-containing alkyl ligand, monosubstituted alkyl/alkoxides of formula $Mo_2R''(OR')_5$ were obtained and the formation of the alkyl ligand R'' was traced to a reductive elimination (alkyl disproportionation)/oxidative addition sequence. For example, in the reaction between $Mo_2Et_2(NMe_2)_4$ and t-BuOD, the eliminated ethane was all protio while the ethyl ligand contained a β-deuterium (eq 1).

$$Mo_2(C_2H_5)_2(NMe_2)_4 + t\text{-BuOD(excess)} \xrightarrow[\text{hexane}]{22\ ^\circ C} Mo_2(CH_2CH_2D)(O\text{-}t\text{-Bu})_5 + C_2H_6 \quad (1)$$

(1) Chisholm, M. H. *Acc. Chem. Res.* **1990**, *23*, 419.
(2) Cotton, F. A.; Walton, R. A. *Multiple Bonds Between Metal Atoms*, 2nd ed.; Oxford University Press: London, 1993.
(3) Huq, F.; Mowat, W.; Shortland, A.; Skapski, A. C.; Wilkinson, G. *J. Chem. Soc., Chem. Commun.* **1971**, 1079.
(4) (a) Chisholm, M. H.; Cotton, F. A.; Reichert, W. W.; Shive, L. *J. Chem. Soc., Chem. Commun.* **1974**, 480. (b) Chisholm, M. H.; Cotton, F. A.; Frenz, B. A.; Reichert, W. W.; Shive, L.; Stults, B. R. *J. Am. Chem. Soc.* **1976**, *98*, 4469.
(5) (a) Chisholm, M. H.; Cotton, F. A.; Extine, M.; Stults, B. R.; Troup, J. M. *J. Am. Chem. Soc.* **1975**, *97*, 1243. (b) Chisholm, M. H.; Extine, M. *J. Am. Chem. Soc.* **1975**, *97*, 5625.
(6) Chisholm, M. H.; Reichert, W. W. *J. Am. Chem. Soc.* **1974**, *96*, 1249.
(7) Akiyama, A.; Chisholm, M. H.; Cotton, F. A.; Extine, M.; Haitko, D. A.; Little, D.; Fanwick, P. E. *Inorg. Chem.* **1979**, *18*, 2266.
(8) Chisholm, M. H.; Corning, J. F.; Folting, K.; Huffman, J. C. *Polyhedron* **1985**, *4*, 383.
(9) Chisholm, M. H.; Parkin, I. P.; Huffman, J. C.; Streib, W. E. *J. Chem. Soc., Chem. Commun.* **1990**, 921.
(10) (a) Chisholm, M. H.; Tatz, R. J. *Organometallics* **1986**, *5*, 1590. (b) Chisholm, M. H.; Eichhorn, B. W.; Folting, K.; Huffman, J. C.; Tatz, R. J. *Organometallics* **1986**, *5*, 1599.

0020-1669/93/1332-3771$04.00/0

Table I. Summary of Crystal Data[a]

	1	2	3	4	5
empirical formula	$Mo_2O_8C_{24}H_{60}$	$C_{40}H_{76}Mo_2O_8$	$Mo_2N_4O_4C_{28}H_{72}$	$Mo_2O_4N_4C_{32}H_{48}$	$Mo_2P_4O_4C_{32}H_{80}$
crystal dimens (mm)	0.24 × 0.24 × 0.28	0.32 × 0.40 × 0.40	0.18 × 0.18 × 0.22	0.15 × 0.15 × 0.15	0.14 × 0.13 × 0.15
space group	*P4/nmm*	*P2/c*	*I4cm*	*P*$\bar{1}$	*Pa*
temp (°C)	−160	−164	−160	−167	−162
a (Å)	12.810(4)	62.232(11)	22.064(5)	18.254(6)	19.441(10)
b (Å)	12.810(4)	10.442(2)	22.064(5)	10.327(2)	11.619(5)
c (Å)	9.869(5)	20.167(3)	16.985(4)	10.076(2)	9.906(4)
α (deg)				70.92(1)	
β (deg)		106.83(1)		103.08(1)	106.41(2)
γ (deg)				104.38(1)	
Z (molecules/cell)	2	12	8	2	2
V (Å^3)	1619.32	12 543.27	8368.93	1716.79	2146.46
calcd density (g/cm^3)	1.371	1.387	1.158	1.440	1.307
wavelength, Å	0.710 69	0.710 69	0.710 69	0.710 69	0.710 69
mol wt	668.61	877.0	720.78	744.64	844.76
linear abs coeff (cm^{-1})	7.920	6.305	6.206	7.505	7.461
no. of reflns					
with $F > 3.0\sigma(F)$	1336				
with $F > 4\sigma(F)$		3380		3765	
with $F > 2.33\sigma(F)$			1378		2652
with $F > 0.0$				0.0311	0.0520
$R(F)$	0.0822	0.1123	0.0636		
$R_w(F)$	0.0985	0.1220	0.0655		

[a] **1** = Mo_2(O-*i*-Pr)$_4$(HO-*i*-Pr)$_4$; **2** = Mo_2(O-c-Pen)(HO-c-Pen); **3** = $Mo_2(OCH_2$-*t*-Bu$)_4(HNMe_2)_4$; **4** = Mo_2(O-*i*-Pr)$_4$(py)$_4$; **5** = $Mo_2(CH_2$-*t*-Bu$)_2(PMe_3)_4$.

By use of the bulky isobutyl ligand, we found that the reactions with alcohols could yield Mo_2^{4+}-containing compounds supported by alkoxide ligands as shown in eq 2.

$$Mo_2(i\text{-Bu})_2(NMe_2)_4 + i\text{-PrOH(excess)} \xrightarrow[\text{hexane}]{22\ ^\circ C} Mo_2(O\text{-}i\text{-Pr})_4(HO\text{-}i\text{-Pr})_4 + Me_3CH + (CH_3)_2C{=}CH_2 + 4HNMe_2 \quad (2)$$

A preliminary aspect of this work was published by way of a communication.[11] We report here our syntheses of a series of Mo_2^{4+} quadruply bonded compounds supported by alkoxide ligands. These are, in fact, the first examples of M–M quadruply bonded compounds supported by strong π-donor alkoxide ligands, and they show some rather interesting properties.

Synthesis

Hydrocarbon solutions of $Mo_2(i\text{-Bu})_2(NMe_2)_4$ react with an excess of 2-propanol in hexene to give Mo_2(O-*i*-Pr)$_4$(HO-*i*-Pr)$_4$ (**1**) as purple crystals; see eq 2. Compound **1** is thermally sensitive and should be stored at −20 °C under dry and oxygen-free N_2. Significant decomposition occurs at room temperature over a period of hours both in solution and in the solid state. One product of decomposition is Mo_2(O-*i*-Pr)$_6$.

In a similar reaction sequence involving cyclopentanol, the purple, crystalline, thermally sensitive compound Mo_2(O-c-Pen)$_4$(HO-c-Pen)$_4$ (**2**) is formed. A reaction involving cyclohexanol also yields a purple microcrystalline precipitate which is believed to be Mo_2(O-c-Hex)$_4$(HO-c-Hex)$_4$, but this compound is essentially insoluble as well as rather thermally sensitive. Also, some Mo_2(O-c-Hex)$_6$ instead of Mo_2(O-c-Hex)$_4$(HO-c-Hex)$_4$ is often formed in this reaction.

Because of the thermal instability of compounds **1** and **2**, we have been unable to obtain satisfactory elemental analysis, though they have been characterized by low-temperature single-crystal X-ray crystallography (see later).

When a reaction between $Mo_2(i\text{-Bu})_2(NMe_2)_4$ and neopentanol is carried out using only 4 equiv of the alcohol and a small amount of dimethylamine is added, the mixed alkoxide/amine complex $Mo_2(OCH_2$-*t*-Bu$)_4(HNMe_2)_4$ (**3**) is obtained (eq 3).

$$Mo_2(i\text{-Bu})_2(NMe_2)_4 + 4t\text{-BuCH}_2\text{OH} + \sim 10HNMe_2 \xrightarrow[\text{hexane}]{22\ ^\circ C} Mo_2(OCH_2\text{-}t\text{-Bu})_4(HNMe_2)_4 + (CH_3)_3CH + (CH_3)_2C{=}CH_2 \quad (3)$$

Compounds **1**–**3** are substitutionally labile, and the reaction between **1** and pyridine leads to the formation of Mo_2(O-*i*-Pr)$_4$(py)$_4$ (**4**), with the liberation of 2-propanol (eq 4).

$$Mo_2(O\text{-}i\text{-Pr})_4(HO\text{-}i\text{-Pr})_4 + \text{py(excess)} \xrightarrow[\text{hexane}]{22\ ^\circ C} Mo_2(O\text{-}i\text{-Pr})_4(py)_4 + 4i\text{-PrOH} \quad (4)$$

Similarly, the dimethylamine ligands in **3** may be displaced by PMe_3 to give $Mo_2(OCH_2$-*t*-Bu$)_4(PMe_3)_4$ (**5**), according to eq 5.

$$Mo_2(OCH_2\text{-}t\text{-Bu})_4(HNMe_2)_4 + PMe_3\text{(excess)} \xrightarrow[\text{hexane}]{22\ ^\circ C} Mo_2(OCH_2\text{-}t\text{-Bu})_4(PMe_3)_4 + 4HNMe_2 \quad (5)$$

The synthetic utility of compound **1** was described elsewhere in its reactions with β-diketones, forming $Mo_2(R'C(O)CRC(O)R')_4$.[12]

Structural Determinations

A summary of the crystal data for the five compounds characterized by X-ray crystallography in this work is given in Table I, and the fractional coordinates for compounds **1**–**5** are given in Tables II–VI, respectively.

Mo_2(O-*i*-Pr)$_4$(HO-*i*-Pr)$_4$ (1). In the space group *P4mnn* there are two crystallographically equivalent molecules in the unit cell. The molecule has crystallographically imposed C_4 symmetry with the C_4 axis coincident with the M–M bond. Consequently, there are only two unique Mo–O distances, Mo(1)–O(7) and Mo(2)–O(3), as shown in the ball-and-stick drawing in Figure 1. The Mo_2O_8 skeleton is eclipsed, as expected for Mo–Mo quadruply bonded complexes, and the O---O distances (O(3) to O(7)), 2.46 Å, together with the arrangement of the Mo–O–C planes, are suggestive of hydrogen bonding across the Mo–Mo quadruple bond. The Mo(1)–O(7) distance, 2.09(1) Å, is notably shorter than Mo(2)–O(3), 2.17(1) Å. Normally one would anticipate

(11) Chisholm, M. H.; Folting, K.; Huffman, J. C.; Tatz, R. J. *J. Am. Chem. Soc.* **1984**, *106*, 1153.

(12) Chisholm, M. H.; Folting, K.; Putilina, E. F. *Inorg. Chem.* **1992**, *31*, 1510.

Table II. Fractional Coordinates and Isotropic Thermal Parameters for $Mo_2(O\text{-}i\text{-}Pr)_4(HO\text{-}i\text{-}Pr)_4$ (**1**)[a]

atom	10^4x	10^4y	10^4z	$10B_{iso}$ (Å^2)	atom	10^4x	10^4y	10^4z	$10B_{iso}$ (Å^2)
Mo(2)	2500*	2500*	1595(2)	15	C(6)	3391(15)	5849(16)	1268(18)	23
Mo(1)	2500*	2500*	3732(2)	9	O(7)	2500*	4127(7)	3909(8)	27
O(3)	2500*	4188(6)	1412(7)	11	C(8)	3527(14)	4678(14)	4533(20)	23
C(4)	3435(12)	4686(13)	906(18)	17	C(9)	3506(16)	5794(15)	4121(20)	27
C(5)	3490(15)	4497(15)	−651(19)	25	C(10)	3393(15)	4561(16)	6075(20)	26

[a] Parameters marked with an asterisk were not varied.

Table III. Fractional Coordinates and Isotropic Thermal Parameters for $Mo_2(O\text{-}c\text{-}C_5H_9)_4(HO\text{-}c\text{-}C_5H_9)_4$ (**2**)

atom	10^4x	10^4y	10^4z	$10B_{iso}$ (Å^2)	atom	10^4x	10^4y	10^4z	$10B_{iso}$ (Å^2)
Mo(1)	1729.6(4)	4016(2)	9(1)	73	C(40)	1799(6)	1955(35)	1843(19)	114(9)
Mo(2)	1621.8(4)	2147(2)	156(1)	77	C(41)	1693(9)	730(55)	1715(26)	191(17)
O(3)	1985(3)	4057(15)	968(7)	74(4)	C(42)	1889(8)	−157(48)	2388(23)	169(14)
C(4)	2222(5)	4213(26)	1006(13)	82(7)	C(43)	2046(7)	510(44)	2281(21)	153(13)
C(5)	2363(5)	3900(29)	1709(15)	96(7)	C(44)	1937(7)	2024(41)	2524(22)	151(12)
C(6)	2319(4)	5042(29)	2148(14)	91(7)	O(45)	1852(3)	1224(16)	−273(8)	83(4)
C(7)	2297(5)	6172(30)	1704(15)	98(8)	C(46)	2041(5)	342(32)	142(16)	104(8)
C(8)	2261(4)	5710(26)	937(13)	83(7)	C(47)	1926(5)	−761(31)	308(15)	102(8)
O(9)	1956(2)	3417(14)	−533(8)	69(4)	C(48)	1932(6)	−1656(33)	−284(18)	116(10)
C(10)	1936(5)	3673(32)	−1316(16)	108(9)	C(49)	2151(7)	−1478(43)	−396(20)	148(12)
C(11)	2131(5)	3040(29)	−1439(15)	99(8)	C(50)	2193(7)	−25(46)	−329(21)	152(12)
C(12)	2343(4)	3809(27)	−1034(13)	85(7)	Mo(51)	4979(1)	9028(4)	1968(2)	93
C(13)	2245(4)	5262(26)	−1015(13)	82(7)	Mo(X)	5175(1)	8810(7)	2584(4)	36
C(14)	1983(5)	5159(29)	−1314(14)	94(7)	O(52)	5199(3)	7468(20)	1963(10)	109(6)
O(15)	1486(3)	4231(16)	−940(8)	83(4)	C(53)	5133(9)	5987(53)	1708(29)	194(16)
C(16)	1283(7)	5230(39)	−1025(19)	126(10)	C(54)	5352(8)	5448(44)	2050(23)	165(14)
C(17)	1097(7)	4899(39)	−1615(22)	142(11)	C(55)	5463(8)	5627(44)	1387(24)	168(14)
C(18)	1124(7)	5652(38)	−2191(20)	139(11)	C(56)	5294(11)	5965(68)	760(32)	99(16)
C(19)	1363(6)	6340(38)	−1951(20)	140(11)	C(57)	5263(12)	4934(77)	947(36)	122(19)
C(20)	1380(6)	6396(39)	−1167(21)	134(11)	C(58)	5105(9)	6382(53)	903(29)	199(17)
O(21)	1507(3)	4896(16)	514(9)	85(4)	O(59)	5213(3)	10349(20)	1923(10)	110(6)
C(22)	1597(7)	5617(42)	1247(22)	144(12)	C(60)	5442(8)	9864(49)	1658(27)	177(15)
C(23)	1438(8)	5856(43)	1573(22)	164(13)	C(61)	5358(11)	9667(69)	1040(38)	105(18)
C(24)	1258(6)	6732(35)	1058(18)	118(10)	C(62)	5265(14)	10951(86)	739(41)	298(27)
C(25)	1413(7)	7450(37)	748(18)	127(11)	C(63)	5529(23)	11437(120)	1302(64)	381(38)
C(26)	1625(7)	6727(45)	883(21)	158(13)	C(64)	5651(12)	11179(75)	1554(36)	234(25)
O(27)	1366(3)	2071(17)	−821(9)	91(5)	O(65)	4743(3)	10462(21)	1729(10)	104(5)
C(28)	1413(7)	1188(42)	−1483(22)	142(12)	C(66)	4754(10)	11780(65)	1651(32)	195(18)
C(29)	1230(8)	1510(39)	−2166(21)	143(12)	C(67)	4777(14)	12127(76)	1003(45)	272(26)
C(30)	1050(8)	1043(46)	−2080(22)	149(13)	C(68)	4569(11)	11685(66)	488(33)	107(17)
C(31)	1082(9)	−70(54)	−1607(27)	185(16)	C(69)	4435(15)	12059(85)	1066(45)	288(28)
C(32)	1325(8)	85(50)	−1188(24)	172(15)	C(70)	4577(14)	12874(76)	1571(41)	257(25)
O(33)	1381(3)	2755(16)	667(8)	81(4)	C(71)	4534(15)	12784(92)	730(46)	149(24)
C(34)	1145(5)	2523(28)	353(14)	90(7)	O(72)	4728(3)	7564(19)	1678(11)	112(6)
C(35)	1004(6)	2948(37)	827(19)	125(10)	C(73)	4551(9)	7999(55)	866(28)	182(16)
C(36)	1029(7)	1923(45)	1379(22)	149(12)	C(74)	4537(11)	6547(61)	532(29)	211(20)
C(37)	1043(7)	685(43)	970(22)	148(13)	C(75)	4319(16)	6568(78)	573(39)	259(27)
C(38)	1110(5)	1032(31)	338(15)	99(8)	C(76)	4196(17)	7437(110)	512(51)	357(34)
O(39)	1854(3)	1934(17)	1152(9)	90(5)	C(77)	4420(10)	8022(50)	1275(27)	188(16)

Table IV. Fractional Coordinates and Isotropic Thermal Parameters for $Mo_2(CH_2\text{-}t\text{-}Bu)_4(HNMe_2)_4$ (**3**)[a]

atom	10^4x	10^4y	10^4z	$10B_{iso}$ (Å^2)	atom	10^4x	10^4y	10^4z	$10B_{iso}$ (Å^2)
Mo(1)	6859(1)	8141*	5161*	22	N(13)	7785(6)	8667(6)	3873(11)	27
Mo(2)	7043(1)	7957*	3851(2)	23	C(14)	7669(12)	9207(12)	3407(16)	65
N(3)	6150(6)	8850*	4891(13)	28	C(15)	8415(10)	8449(10)	3756(17)	61
C(4)	5516(8)	8721(1)	5074(18)	53	O(16)	6449(5)	8551*	3405(10)	23
N(5)	7552(7)	7448*	5614(13)	28	C(17)	6414(10)	8586*	2570(16)	33
C(6)	8084(9)	7665(10)	6019(14)	44	C(18)	5970(8)	9030*	2251(16)	30
O(7)	7479(5)	8829(5)	5409(6)	20	C(19)	5970(10)	9030*	1353(16)	47
C(8)	7559(8)	9120(8)	6115(11)	31	C(20)	5321(9)	8872(10)	2586(15)	50
C(9)	8067(8)	9604(8)	6101(12)	34	O(21)	7707(5)	7293*	4039(11)	26
C(10)	8078(11)	9901(16)	6883(13)	67	C(22)	7973(10)	7027*	3360(16)	40
C(11)	8661(9)	9307(10)	5906(14)	47	C(23)	8449(8)	6551*	3593(20)	41
C(12)	7894(11)	10085(10)	5520(18)	64	C(24)	8163(12)	6052(12)	4073(21)	81

[a] Parameters marked with an asterisk were not varied.

that the shorter distance involved the metal–alkoxide bond and the longer distance the metal–alcohol bond. For **1**, if this were the case, then Mo(1) would be formally Mo(4+) and Mo(2) zerovalent. While this is not out of the question, since this mixed oxidation state is seen in $Mo_2(O\text{-}i\text{-}Pr)_4(dmpe)_2$,[13] where dmpe = $Me_2PCH_2CH_2PMe_2$, it is certainly possible that for **1** the Mo–O distances are an artifact of the space group *P4mnn*. Selected bond distances and angles are given in Table VII.

$Mo_2(O\text{-}c\text{-}Pen)_4(HO\text{-}c\text{-}Pen)_4$ (2). In the space group *C2/c* there are two independent molecules in the unit cell, one of which shows severe disorder. The disordering of a Mo_2 unit within an O_8 cube parallels that seen by Cotton and co-workers for a number of related M_2X_8 species[14] and unfortunately limits the reliability of the metric parameters associated with this molecule. However,

(13) Chisholm, M. H.; Huffman, J. C.; Van Der Sluys, W. G. *J. Am. Chem. Soc.* **1987**, *109*, 2514.

Table V. Fractional Coordinates and Isotropic Thermal Parameters for $Mo_2(O\text{-}i\text{-}Pr)_4(py)_4$ (**4**)

atom	10^4x	10^4y	10^4z	$10B_{iso}$ (Å^2)	atom	10^4x	10^4y	10^4z	$10B_{iso}$ (Å^2)
Mo(1)	9115.8(2)	3324.9(4)	2110.6(4)	20	C(22)	8029(3)	6112(5)	-407(6)	33
Mo(2)	6895.5(2)	2368.3(3)	2007.7(3)	13	O(23)	6741(2)	800(3)	3826(3)	19
O(3)	8286(2)	5030(3)	2811(3)	25	C(24)	6365(3)	-589(4)	4057(4)	23
C(4)	8965(3)	5548(6)	3602(6)	44	C(25)	6295(3)	-1205(5)	5616(5)	34
C(5)	9506(4)	6582(8)	2585(10)	68	C(26)	5591(4)	-740(6)	3149(6)	44
C(6)	8818(5)	6247(11)	4519(11)	90	O(27)	6365(2)	3397(3)	97(3)	19
O(7)	8618(2)	2141(3)	1456(3)	27	C(28)	5693(2)	3962(4)	-228(4)	18
C(8)	9274(3)	2535(5)	794(6)	30	C(29)	4996(3)	2813(5)	4(6)	29
C(9)	9473(3)	1238(6)	696(7)	38	C(30)	5626(3)	4903(5)	-1734(5)	28
C(10)	9946(3)	3306(7)	1605(9)	56	N(31)	6954(2)	874(3)	894(3)	18
N(11)	8424(2)	2035(4)	4312(4)	26	C(32)	7381(3)	-111(4)	1481(5)	22
C(12)	8213(3)	2248(5)	5406(5)	29	C(33)	7407(3)	-1087(5)	834(5)	28
C(13)	8383(3)	1500(6)	6765(6)	37	C(34)	6974(3)	-1051(5)	-480(5)	31
C(14)	8788(4)	449(6)	7081(6)	49	C(35)	6540(3)	-39(5)	-1102(5)	29
C(15)	8997(4)	190(7)	5969(6)	51	C(36)	6544(3)	907(5)	-409(5)	23
C(16)	8819(3)	994(6)	4629(6)	39	N(37)	6583(2)	3646(3)	3113(3)	16
N(17)	7962(2)	4699(4)	-78(4)	30	C(38)	6270(2)	3054(5)	4303(5)	21
C(18)	7851(3)	4165(6)	-1187(5)	33	C(39)	6056(3)	3797(5)	5019(5)	27
C(19)	7722(3)	4878(6)	-2501(7)	46	C(40)	6167(3)	5237(5)	4500(5)	26
C(20)	7768(4)	6326(7)	-2856(6)	52	C(41)	6487(2)	5861(4)	3284(5)	21
C(21)	7925(4)	6893(6)	-1715(7)	49	C(42)	6693(2)	5051(4)	2634(4)	18

the other molecule is not so disordered, and a view of it is shown in Figure 2. Selected bond distances and angles are given in Table VIII. Particularly pertinent to the question of the nature of the hydrogen bonding are the Mo–O distances, the O---O distances, and the Mo–Mo–O angles. For compound **2** these are shown in Figure 3, where it becomes apparent that the X-ray structural determination cannot resolve the difference between alkoxide and alcoholate ligands. This situation may be contrasted with the recently reported structures of $M_2(O\text{-}i\text{-}Pr)_8(HO\text{-}i\text{-}Pr)_2$ (M = Zr, Ce),[15] where low-temperature crystallography revealed significant differences in the Mo–OR and M–O(H)R bonds associated with asymmetric hydrogen bonds of the type shown schematically in **A**. In the Zr- and Ce-containing compounds,

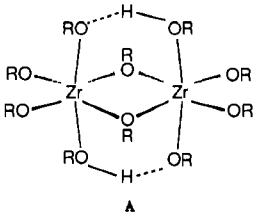

A

the M–M distances are nonbonding, 3.50 Å for M = Zr and 3.77 Å for M = Ce. The hydrogen bonding depicted in **A** thus leads to M–M–O angles that are less than 90°. In both compounds the O---O separation falls in the range 2.76–2.78 Å, notably longer than in compounds **1** and **2**, which have short M–M distances, *ca.* 2.10 Å, and O---O distances of *ca.* 2.40 Å.

We shall return to the question of symmetric *vs* asymmetric hydrogen bonding in the $Mo_2(OR)_4(HOR)_4$ compounds later in this paper.

$Mo_2(OCH_2\text{-}t\text{-}Bu)_4(HNMe_2)_4$ (3). In the space group *I4cm* there is only one unique molecule in the unit cell. A ball-and-stick drawing of the molecule is given in Figure 4. The molecule has a crystallographically imposed mirror plane of symmetry that contains N(3), Mo(1), N(5), O(10), Mo(2), and O(21). The hydrogen atoms were located crystallographically but are omitted from Figure 4 for clarity. The orientation of the amine N–H moieties allows for hydrogen bonding across the Mo–Mo bond. The distances N(3)–O(16) and N(5)–O(21) are 2.65 and 2.71 Å, respectively. Pertinent metal–ligand distances and angles are given in Table IX.

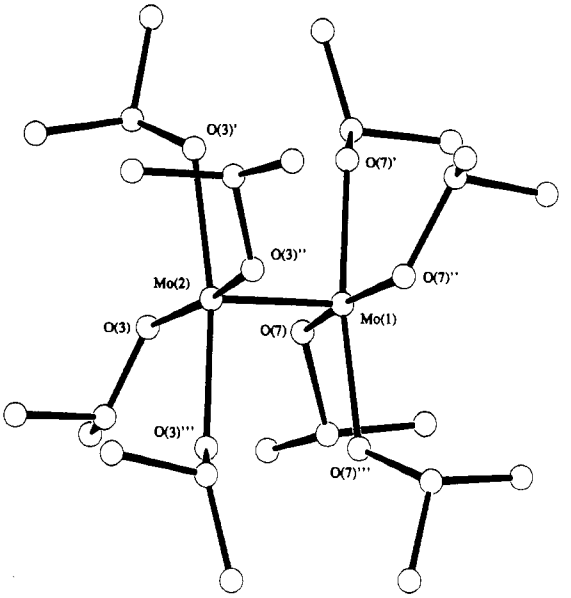

Figure 1. Ball-and-stick drawing of $Mo_2(O\text{-}i\text{-}Pr)_4(HO\text{-}i\text{-}Pr)_4$ (**1**).

In this structure the hydrogen bond is clearly asymmetric, being of the form N–H---O, and this results in somewhat longer Mo–O distances when compared to those of compounds **1** and **2**.

$Mo_2(O\text{-}i\text{-}Pr)_4(py)_4$ (4). In the space group $P\bar{1}$ there is one unique molecule, a view of which is given in Figure 5. Selected bond distances and angles are given in Table X. Particularly noteworthy in this structure are the shorter Mo–O distances, 2.03 Å (average), and the rather long Mo–Mo distance of 2.195(1) Å for a quadruple bond. The Mo–O–C angles range from 125 to 132°. Although these Mo–O distances are referred to as short when compared to those seen for compounds **1** and **2**, they are notably longer than those seen in Mo_2^{6+}-containing compounds such as $Mo_2(O\text{-}i\text{-}Pr)_6(py)_2$,[16] where Mo–O = 1.95 Å (average).

$Mo_2(OCH_2\text{-}t\text{-}Bu)_4(PMe_3)_4$ (5). In the space group *Pa* the molecule has no crystallographically imposed element of symmetry. As in compound **4**, the alkoxide ligands are mutually trans at each metal center and the eclipsed geometry leads to syn Mo–P and Mo–O bonds. Although this could be due to steric factors, as is presumably the case for $Mo_2X_4(PMe_3)_4$ compounds where X = halide,[2] in the case of compounds **4** and **5** this arrangement of ligands minimizes O---O repulsive interactions

(14) (a) Cotton, F. A.; Frenz, B. A.; Stults, B. R.; Webb, T. R. *J. Am. Chem. Soc.* **1976**, *98*, 2768. (b) Cotton, F. A.; Daniels, L. M.; Vidyasagar, K. *Polyhedron* **1988**, *7*, 1667. (c) Cotton, F. A.; Daniels, L. M. *Inorg. Chim. Acta* **1988**, *142*, 255.

(15) (a) Vaarstra, B. A.; Huffman, J. C.; Gradeff, P. S.; Hubert-Pfalzgraf, L. G.; Daran, J.-C.; Parraud, S.; Yunlu, K.; Caulton, K. G. *Inorg. Chem.* **1990**, *29*, 3126. (b) Huggins, B. A.; Ellis, P. D.; Gradeff, P. S.; Vaarstra, B. A.; Yunla, K.; Huffman, J. C.; Caulton, K. G. *Inorg. Chem.* **1991**, *30*, 1720.

(16) Chisholm, M. H. *Polyhedron* **1983**, *2*, 681.

Table VI. Fractional Coordinates and Isotropic Thermal Parameters for $Mo_2(CH_2\text{-}t\text{-}Bu)_2(PMe_3)_4$ (**5**)[a]

atom	10^4x	10^4y	10^4z	$10B_{iso}$ (Å^2)	atom	10^4x	10^4y	10^4z	$10B_{iso}$ (Å^2)
Mo(1)	6181*	4171(1)	10901*	16	C(22)	7675(21)	6674(34)	14928(40)	61(9)
Mo(2)	6801(2)	2262(1)	10889(5)	16	C(23)	8595(26)	7413(44)	13993(53)	71(13)
P(3)	5907(9)	4434(10)	12248(10)	26	C(24)	8772(22)	5541(36)	15111(44)	72(10)
C(4)	4965(23)	3796(37)	11530(43)	55(10)	O(25)	6155(11)	4818(20)	9014(23)	26(5)
C(5)	6122(16)	3821(26)	14008(31)	27(6)	C(26)	5549(15)	5396(24)	8672(28)	50(6)
C(6)	5750(12)	5987(20)	12546(23)	20(4)	C(27)	5617(15)	6623(24)	8035(30)	34(6)
P(7)	7728(4)	4406(9)	9533(12)	35	C(28)	6134(17)	7309(28)	9125(33)	56(7)
C(8)	7420(20)	4047(32)	7784(39)	47(9)	C(29)	4831(20)	7159(31)	7660(38)	50(8)
C(9)	8613(15)	3934(24)	10013(30)	33(5)	C(30)	5807(19)	6350(32)	6647(37)	38(8)
C(10)	7987(26)	5833(40)	9273(52)	73(13)	O(31)	7485(13)	1666(20)	9759(25)	35(6)
P(11)	7850(6)	2017(9)	13140(13)	30	C(32)	7400(14)	782(23)	8984(29)	39(5)
C(12)	8725(20)	2316(30)	13192(37)	43(8)	C(33)	7988(19)	−9(30)	8927(37)	36(7)
C(13)	7772(15)	2528(23)	14857(29)	21(6)	C(34)	8585(46)	823(73)	8634(9)	139(29)
C(14)	8124(16)	635(26)	13513(32)	38(6)	C(35)	8377(18)	−647(28)	10226(34)	61(7)
P(15)	5783(5)	1996(10)	8666(11)	24	C(36)	7742(15)	−833(24)	7710(29)	44(5)
C(16)	5766(19)	2652(30)	7070(38)	36(8)	O(37)	6074(12)	1634(20)	11759(24)	23(5)
C(17)	4907(18)	2608(29)	8789(35)	38(7)	C(38)	5977(18)	538(29)	11956(36)	58(7)
C(18)	5651(14)	408(23)	8074(28)	25(5)	C(39)	5634(17)	58(27)	13069(35)	22(6)
O(19)	7516(12)	4754(22)	12631(24)	24(5)	C(40)	6193(20)	0(33)	14485(38)	68(9)
C(20)	7933(15)	5736(25)	12816(29)	50(6)	C(41)	5389(27)	−1170(43)	12651(53)	104(12)
C(21)	8210(15)	6337(24)	14115(30)	27(6)	C(42)	5089(15)	802(24)	13332(30)	34(5)

[a] Parameters marked with an asterisk were not varied.

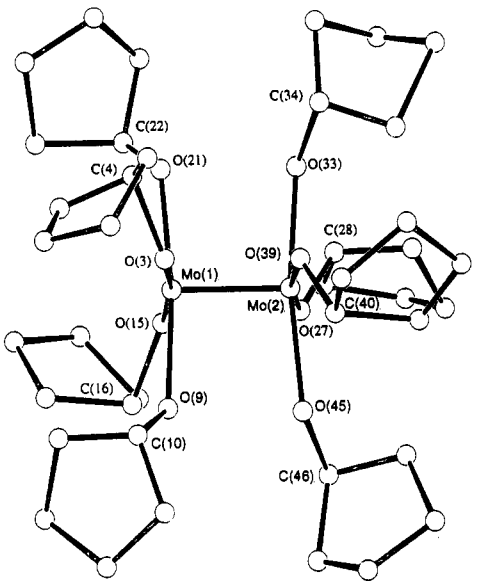

Figure 2. Ball-and-stick drawing of $Mo_2(O\text{-}c\text{-}Pen)_4(HO\text{-}c\text{-}Pen)_4$ (**2**).

Table VII. Selected Bond Distances (Å) and Bond Angles (deg) for the $Mo_2(O\text{-}i\text{-}Pr)_4(HO\text{-}i\text{-}Pr)_4$ Molecule

Distances			
Mo(2)–Mo(1)	2.110(3)	C(4)–C(5)	1.557(25)
Mo(2)–O(3)	2.170(7)	C(4)–C(6)	1.533(26)
Mo(1)–O(7)	2.092(9)	C(5)–C(5)	1.82(4)
O(3)–C(4)	1.446(16)	C(8)–C(9)	1.487(28)
O(7)–C(8)	1.614(17)	C(8)–C(10)	1.54(3)
Angles			
Mo(1)–Mo(2)–O(3)	94.76(20)	O(3)–C(4)–C(5)	108.0(14)
O(3)–Mo(2)–O(3)	89.61(3)	O(3)–C(4)–C(6)	108.5(13)
Mo(2)–Mo(1)–O(7)	94.76(23)	C(5)–C(4)–C(6)	112.5(14)
O(7)–Mo(1)–O(7)	94.76(23)	C(4)–C(5)–C(5)	98.2(9)
Mo(2)–O(3)–C(4)	117.9(7)	O(7)–C(8)–C(9)	107.5(15)
C(4)–O(3)–C(4)	111.8(13)	O(7)–C(8)–C(10)	104.1(12)
Mo(1)–O(7)–C(8)	117.9(8)	C(9)–C(8)–C(10)	111.2(15)
C(8)–O(7)–C(8)	109.1(14)		

which might otherwise arise from the short Mo–Mo distance (there are no hydrogen bonds in **4** and **5**). Selected bond distances and angles are given in Table XI. The Mo–O distances appear in pairs of short (1.99 Å) and long (2.08 Å) at each metal center. However, the quality of the structural determination does allow us to place a true significance on these values. That is to say, their distances overlap by the criteria of 3σ and again an average

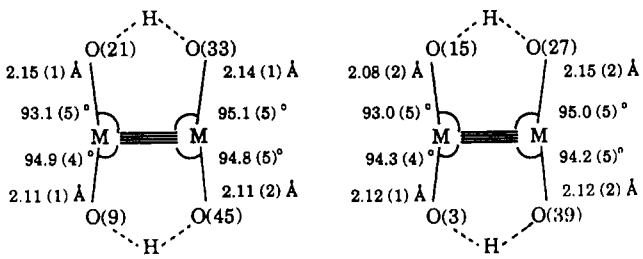

Figure 3. Bond distances and angles for the M–M and M–O bonds of $Mo_2(O\text{-}c\text{-}Pen)_4(HO\text{-}c\text{-}Pen)_4$ (**2**).

Table VIII. Selected Bond Distances (Å) and Bond Angles (deg) for the $Mo_2(O\text{-}c\text{-}C_5H_9)_4(HO\text{-}c\text{-}C_5H_9)_4$ Molecule

Distances			
Mo(1)–Mo(2)	2.113(3)	O(9)–C(10)	1.57(3)
Mo(1)–O(3)	2.118(15)	O(15)–C(16)	1.61(4)
Mo(1)–O(9)	2.113(15)	O(21)–C(22)	1.61(4)
Mo(1)–O(15)	2.082(16)	O(27)–C(28)	1.72(4)
Mo(1)–O(21)	2.150(17)	O(33)–C(34)	1.44(3)
Mo(2)–O(27)	2.146(17)	O(39)–C(40)	1.53(3)
Mo(2)–O(33)	2.144(16)	O(45)–C(46)	1.54(3)
Mo(2)–O(39)	2.119(17)	O(52)–C(53)	1.64(5)
Mo(2)–O(45)	2.110(17)		
Angles			
Mo(2)–Mo(1)–O(3)	94.3(4)	Mo(1)–Mo(2)–O(27)	95.0(5)
Mo(2)–Mo(1)–O(9)	94.9(4)	Mo(1)–Mo(2)–O(33)	95.1(5)
Mo(2)–Mo(1)–O(15)	93.0(5)	Mo(1)–Mo(2)–O(39)	94.2(5)
Mo(2)–Mo(1)–O(21)	93.1(5)	Mo(1)–Mo(2)–O(45)	94.8(5)
O(3)–Mo(1)–O(9)	92.4(6)	O(27)–Mo(2)–O(33)	90.9(6)
O(3)–Mo(1)–O(15)	172.6(6)	O(27)–Mo(2)–O(39)	170.8(7)
O(3)–Mo(1)–O(21)	88.5(6)	O(27)–Mo(2)–O(45)	91.1(6)
O(9)–Mo(1)–O(15)	88.6(6)	O(33)–Mo(2)–O(39)	87.4(6)
O(9)–Mo(1)–O(21)	171.9(6)	O(33)–Mo(2)–O(45)	169.8(6)
O(15)–Mo(1)–O(21)	89.5(6)	O(39)–Mo(2)–O(45)	89.0(7)

Mo–O distance is 2.03 Å. The Mo–O–C angles range from 125 to 134°. Notable again is the long Mo–Mo distance, 2.218(2) Å, which may be compared with the Mo–Mo triple-bond distance of 2.222(2) Å in $Mo_2(OCH_2\text{-}t\text{-}Bu)_6$.[17]

General Comments on the Structural Parameters. A summary of Mo–Mo and Mo–O distances for the five structurally characterized compounds is given in Table XII. For the sake of comparison, we include structural parameters for some related Mo_2^{4+}-containing compounds supported by perfluorophenoxide

(17) Chisholm, M. H.; Cotton, F. A.; Murillo, C. A.; Reichert, W. W. *Inorg. Chem.* **1977**, *16*, 1801.

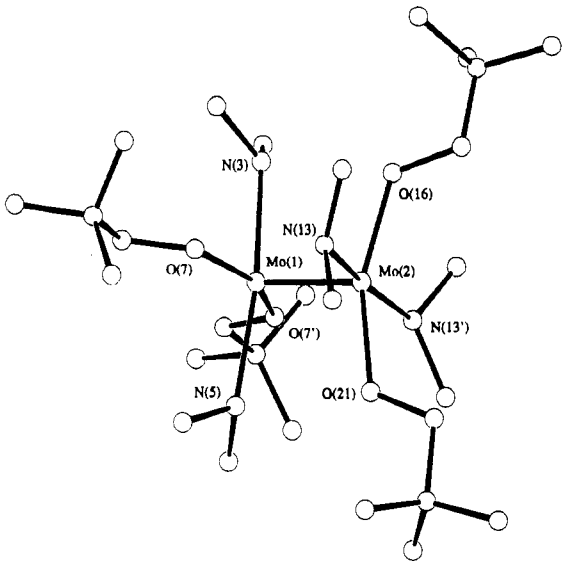

Figure 4. Ball-and-stick drawing of $Mo_2(OCH_2\text{-}t\text{-}Bu)_4(HNMe_2)_4$ (**3**).

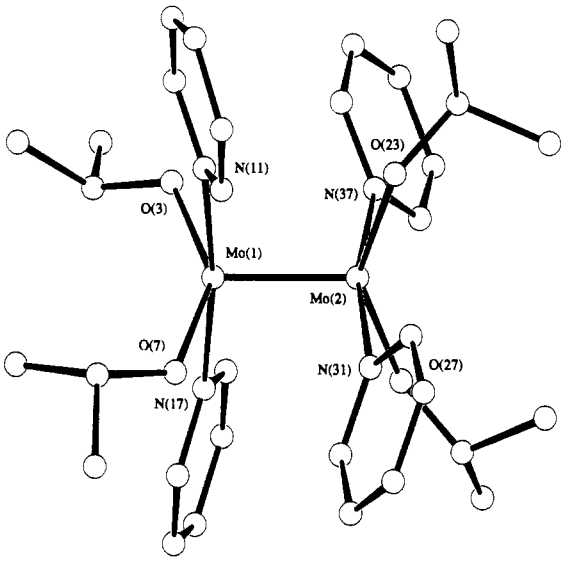

Figure 5. Ball-and-stick drawing of $Mo_2(O\text{-}i\text{-}Pr)_4(py)_4$ (**4**).

ligands that were prepared by Cotton and co-workers.[18] The following general points are worthy of note.

1. The presence of hydrogen bonding across the Mo–Mo bond produces longer Mo–O distances and shorter Mo–Mo distances.

2. In the absence of hydrogen bonding between the alkoxide ligands, the Mo–Mo distances are abnormally long for compounds containing Mo–Mo quadruple bonds.

3. In all of the compounds reported, the Mo–O–C angles fall in a narrow range of *ca.* 125–135°. None are approaching linearity. To a first approximation, the oxygen atoms may be viewed as sp^2 hybridized.

We propose that the relatively long Mo–Mo distances in compounds **4** and **5** result from the unfavorable filled–filled O p_π–Mo d_π interactions. This leads to a weakening of the M–M π and δ bonding. If the Mo–O–C plane were to be aligned so as to contain the Mo–Mo axis, then the O p_π orbital would specifically interact with only the Mo δ orbitals. However, the alignment of the Mo–O–C planes in all cases is such as to allow for an interaction with both Mo–Mo δ and π orbitals. A view of the $Mo_2(O\text{-}c\text{-}Pen)_4(HO\text{-}c\text{-}Pen)_4$ molecule down the Mo–Mo axis is displayed in Figure 7, which clearly shows the disposition of the Mo–O–C planes with respect to the Mo–Mo axis. The fact that the Mo–Mo distances in compounds **4** and **5** are *ca.* 2.20 Å indicates that Mo d_π–Mo d_π bonding is more important than Mo d_π–O p_π bonding in these molecules. Nevertheless, the effect of the filled O p_π orbitals leads to unusually long Mo–Mo distances (for Mo–Mo quadruple bonds) and relatively long Mo–O distances and Mo–O–C angles that are close to 120°.

Table IX. Selected Bond Distances (Å) and Bond Angles (deg) for the $Mo_2(OCH_2\text{-}t\text{-}Bu)_4(HNMe_2)_4$ Molecule

Distances			
Mo(1)–Mo(2)	2.133(3)	O(7)–C(8)	1.37(3)
Mo(1)–O(7)	2.085(8)	O(16)–C(17)	1.42(3)
Mo(1)–N(3)	2.260(11)	O(21)–C(22)	1.42(3)
Mo(1)–N(5)	2.293(11)	N(13)–C(14)	1.45(2)
Mo(2)–O(16)	2.073(12)	N(13)–C(15)	1.49(2)
Mo(2)–O(21)	2.076(11)	N(3)–C(4)	1.46(2)
Mo(2)–N(13)	2.269(13)	N(5)–C(6)	1.44(3)
Angles			
Mo(2)–Mo(1)–O(7)	102.0(3)	N(13)–Mo(2)–N(13)′	172.9(8)
Mo(2)–Mo(1)–N(3)	93.9(4)	Mo(1)–O(7)–C(8)	127.0(8)
Mo(2)–Mo(1)–N(5)	94.0(6)	Mo(2)–O(16)–C(17)	121.0(8)
O(7)–Mo(1)–O(7)′	156.0(12)	Mo(2)–O(21)–C(22)	121.7(14)
O(7)–Mo(1)–N(3)	89.5(9)	Mo(1)–N(3)–C(4)	119.0(10)
O(7)–Mo(1)–N(5)	88.9(8)	C(4)–N(3)–C(4)′	109.2(11)
N(3)–Mo(1)–N(5)	172.1(9)	Mo(1)–N(5)–C(6)	118.8(17)
Mo(1)–Mo(2)–O(16)	101.0(4)	Mo(1)–N(5)–C(6)′	118.8(12)
Mo(1)–Mo(2)–O(21)	101.5(3)	C(6)–N(5)–C(6)′	109.2(19)
Mo(1)–Mo(2)–N(13)	93.6(3)	Mo(2)–N(13)–C(14)	118.2(7)
O(16)–Mo(2)–O(21)	157.5(8)	Mo(2)–N(13)–C(15)	117.4(11)
O(16)–Mo(2)–N(13)	89.6(8)	C(14)–N(13)–C(15)	110.8(18)
O(21)–Mo(2)–N(13)	89.0(8)	O(7)–C(8)–C(9)	113.8(17)

Table X. Selected Bond Distances (Å) and Bond Angles (deg) for the $Mo_2(O\text{-}i\text{-}Pr)_4(py)_4$ Molecule

Distances			
Mo(1)–Mo(2)	2.195(1)	O(23)–C(24)	1.395(5)
Mo(1)–O(3)	2.033(3)	O(27)–C(28)	1.414(5)
Mo(1)–O(7)	2.032(3)	N(11)–C(12)	1.344(6)
Mo(1)–N(11)	2.210(4)	N(11)–C(16)	1.354(6)
Mo(1)–N(17)	2.197(4)	N(17)–C(18)	1.355(6)
Mo(2)–O(23)	2.031(3)	N(17)–C(22)	1.364(6)
Mo(2)–O(27)	2.026(3)	N(31)–C(32)	1.337(5)
Mo(2)–N(31)	2.218(3)	N(31)–C(36)	1.350(5)
Mo(2)–N(37)	2.220(3)	N(37)–C(38)	1.341(5)
O(3)–C(4)	1.400(6)	N(37)–C(42)	1.349(5)
O(7)–C(8)	1.410(5)		
Angles			
Mo(2)–Mo(1)–O(3)	108.0(1)	O(23)–Mo(2)–N(37)	84.5(1)
Mo(2)–Mo(1)–O(7)	106.6(1)	O(27)–Mo(2)–N(31)	84.9(1)
Mo(2)–Mo(1)–N(11)	93.6(1)	O(27)–Mo(2)–N(37)	83.2(1)
Mo(2)–Mo(1)–N(17)	93.4(1)	N(31)–Mo(2)–N(37)	168.1(1)
O(3)–Mo(1)–O(7)	145.4(1)	Mo(1)–O(3)–C(4)	125.0(3)
O(3)–Mo(1)–N(11)	90.3(1)	Mo(1)–O(7)–C(8)	129.1(3)
O(3)–Mo(1)–N(17)	88.4(1)	Mo(2)–O(23)–C(24)	131.7(2)
O(7)–Mo(1)–N(11)	87.7(1)	Mo(2)–O(27)–C(28)	129.3(2)
O(7)–Mo(1)–N(17)	89.4(1)	Mo(1)–N(11)–C(12)	120.5(3)
N(11)–Mo(1)–N(17)	172.9(1)	Mo(1)–N(11)–C(16)	122.6(3)
Mo(1)–Mo(2)–O(23)	109.0(1)	Mo(1)–N(11)–C(12)	119.7(3)
Mo(1)–Mo(2)–O(27)	106.4(1)	Mo(1)–N(17)–C(18)	123.5(3)
Mo(1)–Mo(2)–N(31)	95.1(1)	Mo(2)–N(31)–C(32)	122.1(3)
Mo(1)–Mo(2)–N(37)	96.9(1)	Mo(2)–N(31)–C(36)	121.0(3)
O(23)–Mo(2)–O(27)	144.6(1)	Mo(2)–N(37)–C(38)	121.4(3)
O(23)–Mo(2)–N(31)	91.2(1)	Mo(2)–N(37)–C(42)	122.5(3)

Solution Characterization Data. Compounds **1**–**5** have been characterized by infrared spectroscopy (see Experimental Section) and by NMR and UV–visible spectroscopy.

By ^1H NMR spectroscopy compounds **1** and **2** show only one OR resonance and a signal at *ca.* 12.5 ppm assignable to the hydroxyl hydrogen-bonded proton. In part, this downfield shift of the RO*H* proton can be ascribed to the large diamagnetic anisotropy of the Mo–Mo quadruple bond.[19] The resonance for the hydroxyl proton in $Zr_2(O\text{-}i\text{-}Pr)_8(HO\text{-}i\text{-}Pr)_2$, for example, is found at δ 6.3 ppm.[15] We have found that, on lowering of the

(18) (a) Abbott, R. G.; Cotton, F. A.; Falvello, L. R. *Inorg. Chem.* **1990**, *29*, 514. (b) Cotton, F. A.; Wiesinger, K. J. *Inorg. Chem.* **1991**, *30*, 750.

(19) (a) San Filippo, J., Jr. *Inorg. Chem.* **1972**, *11*, 3140. (b) Cotton, F. A.; Kitagawa, S. *Polyhedron* **1988**, *7*, 1673.

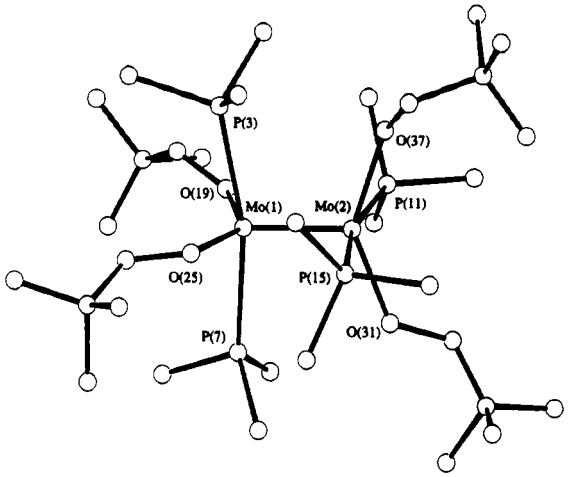

Figure 6. Ball-and-stick drawing of $Mo_2(OCH_2\text{-}t\text{-}Bu)_4(PMe_3)_4$ (**5**).

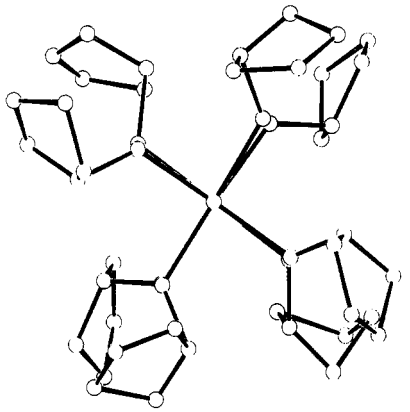

Figure 7. View of $Mo_2(O\text{-}c\text{-}Pen)_4(HO\text{-}c\text{-}Pen)_4$ (**2**) down the Mo–Mo axis.

temperature from +22 to –60 °C, compound **1** (when dissolved in toluene-d_8) showed a downfield shift of 0.2 ppm/20 °C. See Figure 8. We were not able to freeze out hydrogen atom transfer between the alcohol and the alkoxide ligands.

As was noted earlier in the discussion of the crystallographic data, there is an uncertainty as to whether or not the hydroxyl protons are symmetrically or asymmetrically bridging. The nature of hydrogen bonding between oxygen atoms is one of the more fundamental aspects of chemistry, and it is well-known that there are two limiting situations: (1) There is an asymmetric hydrogen bond and thus a significant (albeit relatively small) barrier to hydrogen atom transfer, and (2) the hydrogen bond is symmetrical and thus there exists only one potential well.[20]

In order to address this question, we prepared the deuterated analogue. The isotope chemical shift difference for the three isotopes of hydrogen, ^1H, ^2H, and ^3H, have been considered from both a theoretical and an experimental standpoint. The value $\Delta\delta(^1H,^xH) = \delta(^1H) - \delta(^xH)$ where $x = 2$ or 3 may be positive or negative (and also zero). Positive values of $\Delta\delta(^1H,^xH)$ are indicative of an asymmetric hydrogen bridge, as was seen in the crystallographically characterized compounds $M_2(O\text{-}i\text{-}Pr)_8(HO\text{-}i\text{-}Pr)_2$.[15] For M = Ce,[15b] low-temperature ^2H NMR spectroscopic studies revealed that it was not possible to freeze out the alkoxide and alcoholate ligands even at 104 K. In our studies of $Mo_2(O\text{-}i\text{-}Pr)_4(HO\text{-}i\text{-}Pr)_4$ and $Mo_2(O\text{-}i\text{-}Pr\text{-}d_7)_4(DO\text{-}i\text{-}Pr\text{-}d_7)_4$, we observe a negative value for $\Delta\delta(^1H,^2H)$ of –0.58 ppm, which indicates a symmetrical hydrogen bond. This is consistent with the structural data observed for the compound $Mo_2(O\text{-}c\text{-}Pen)_4(HO\text{-}c\text{-}Pen)_4$ and in more general terms with the fact that symmetrical hydrogen bonds between oxygen atoms are normally seen for short O---O distances (2.50 Å or less), such as in **1** and **2**, whereas in compounds with longer O---O distances of say 2.7 Å or longer, as in $M_2(O\text{-}i\text{-}Pr)_8(HO\text{-}i\text{-}Pr)_2$[15] (shown in **A**), there are asymmetric hydrogen bonds.

Table XI. Selected Bond Distances (Å) and Bond Angles (deg) for the $Mo_2(CH_2\text{-}t\text{-}Bu)_4(PMe_3)_4$ Molecule

		Distances	
Mo(1)–Mo(2)	2.2183(21)	P(3)–C(6)	1.867(25)
Mo(1)–P(3)	2.519(14)	P(7)–C(8)	1.72(4)
Mo(1)–P(7)	2.528(10)	P(7)–C(9)	1.74(3)
Mo(1)–O(19)	1.980(24)	P(7)–C(10)	1.77(5)
Mo(1)–O(25)	2.088(22)	P(11)–C(12)	1.72(4)
Mo(2)–P(11)	2.578(12)	P(11)–C(13)	1.85(3)
Mo(2)–P(15)	2.530(9)	P(11)–C(14)	1.70(3)
Mo(2)–O(31)	2.083(25)	P(15)–C(16)	1.75(4)
Mo(2)–O(37)	1.991(23)	P(15)–C(17)	1.88(3)
P(3)–C(4)	1.92(40)	P(15)–C(18)	1.93(3)
P(3)–C(5)	1.82(3)		
		Angles	
Mo(2)–Mo(1)–P(3)	96.5(3)	P(15)–Mo(2)–O(37)	81.7(7)
Mo(2)–Mo(1)–P(7)	96.70(28)	O(31)–Mo(2)–O(37)	138.6(6)
Mo(2)–Mo(1)–O(19)	110.6(7)	Mo(1)–P(3)–C(4)	119.8(13)
Mo(2)–Mo(1)–O(25)	110.5(7)	Mo(1)–P(3)–C(5)	117.1(11)
P(3)–Mo(1)–P(7)	166.84(20)	Mo(1)–P(3)–C(6)	111.8(9)
P(3)–Mo(1)–O(19)	85.0(7)	Mo(1)–P(7)–C(8)	114.7(13)
P(3)–Mo(1)–O(25)	94.7(6)	Mo(1)–P(7)–C(9)	127.4(11)
P(7)–Mo(1)–O(19)	90.8(7)	Mo(1)–P(7)–C(10)	116.7(16)
P(7)–Mo(1)–O(25)	80.2(6)	Mo(2)–P(11)–C(12)	122.4(13)
O(19)–Mo(1)–O(25)	138.6(5)	Mo(2)–P(11)–C(13)	120.6(10)
Mo(1)–Mo(2)–P(11)	95.7(3)	Mo(2)–P(11)–C(14)	114.5(12)
Mo(1)–Mo(2)–P(15)	97.7(3)	Mo(2)–P(15)–C(16)	123.0(13)
Mo(1)–Mo(2)–O(31)	108.9(7)	Mo(2)–P(15)–C(17)	113.4(11)
Mo(1)–Mo(2)–O(37)	112.0(7)	Mo(2)–P(15)–C(18)	112.7(9)
P(11)–Mo(2)–P(15)	166.61(16)	Mo(1)–O(19)–C(20)	129.1(19)
P(11)–Mo(2)–O(31)	87.7(7)	Mo(1)–O(25)–C(26)	134.1(19)
P(11)–Mo(2)–O(37)	94.0(7)	Mo(2)–O(31)–C(32)	127.1(20)
P(15)–Mo(2)–O(31)	87.3(7)	Mo(2)–O(37)–C(38)	124.8(21)

All of the compounds are colored and show absorptions in the visible region of the spectrum. In particular, the $Mo_2(OR)_4(HOR)_4$ compounds are purple while the phosphine adduct $Mo_2(OCH_2\text{-}t\text{-}Bu)_4(PMe_3)_4$ is green and the pyridine adduct $Mo_2(O\text{-}i\text{-}Pr)_4(py)_4$ is brown. For the purple compounds **1** and **2** the visible absorption at *ca.* 560 nm has a molar extinction coefficient of *ca.* 600 M^{-1} cm^{-1}. See Figure 9. Quite probably this is assignable to the metal-based δ to δ^* singlet transition.[21] There are higher energy absorptions in the UV–visible region with much larger molar extinction coefficients, and it is likely that these are due to fully allowed charge-transfer transitions, O p_π to metal δ^* or π^*. For $Mo_2(O\text{-}i\text{-}Pr)_4(py)_4$ we did not locate a band in this region, perhaps because it was obscured by a tailing of the higher energy absorption into the visible region of the spectrum. Data are recorded in the Experimental Section.

The compounds were also examined by cyclic voltametry in THF with $(n\text{-}Bu)_4N^+PF_6^-$ (0.2 M) and showed irreversible oxidation behavior. The compounds are readily oxidized, as was evident from the oxidation potential of **1** at –1.27 V *vs* ferrocene. This may be compared with the first reversible oxidation of $Mo_2(O_2C\text{-}t\text{-}Bu)_4$,[22] which occurs at –0.04 V *vs* ferrocene, and those for the oxidation of $Mo_2(OC_6H_3\text{-}3,5\text{-}Me_2)_4L_4$, which occur at –1.29 and –0.65 V (L = PMe_3) and –1.04 and –0.58 V (L = $HNMe_2$).[23]

Studies of the Alcohol Exchange with Compound 1. Since compounds **1** and **2** are substitutionally labile and are good starting materials for the synthesis of other Mo_2^{4+}-containing compounds, it was of interest to examine the nature of the substitution reaction.

(20) (a) Singh, T. R.; Wood, J. L. *J. Chem. Phys.* **1969**, *50*, 3572. (b) Altman, L. J.; Laungani, D.; Gunnarson, G.; Wennerstrom, H.; Forsen, S. *J. Am. Chem. Soc.* **1978**, *100*, 8264. (c) Ditchfield, R. *J. Chem. Phys.* **1976**, *65*, 3123.

(21) Hopkins, M. D.; Gray, H. G.; Miskowski, V. M. *Polyhedron* **1987**, *6*, 605.

(22) Cayton, R. H.; Chisholm, M. H.; Huffman, J. C.; Lobkovsky, E. B. *J. Am. Chem. Soc.* **1991**, *113*, 8709.

(23) Coffindaffer, T. W.; Niccolai, G. P.; Powell, D.; Rothwell, I. P.; Huffman, J. C. *J. Am. Chem. Soc.* **1985**, *107*, 3572.

Table XII. Summary of M–M and M–Ligand Distances (Å) for Compounds 1–5

compd	Mo(1)–Mo(2)	Mo(1)–ligand		Mo(2)–ligand		ref
$Mo_2(O\text{-}i\text{-}Pr)_4(HO\text{-}i\text{-}Pr)_4$ (1)	2.11	–O(7)	2.09	–O(3)	2.27	this work
$Mo_2(O\text{-}c\text{-}Pen)_4(HO\text{-}c\text{-}Pen)_4$ (2)	2.13	–O(3)	2.12	–O(27)	2.15	this work
		–O(9)	2.11	–O(33)	2.14	
		–O(15)	2.08	–O(39)	2.12	
		–O(21)	2.15	–O(45)	2.11	
$Mo_2(OCH_2\text{-}t\text{-}Pen)_4(HNMe_2)_4$ (3)	2.13	–O(7)	2.08	–O(16)	2.07	this work
		–N(3)	2.26	–O(21)	2.08	
		–N(5)	2.29	–N(13)	2.27	
$Mo_2(O\text{-}i\text{-}Pr)_4(py)_4$ (4)	2.19	–O(3)	2.03	–O(23)	2.03	this work
		–O(7)	2.03	–O(27)	2.03	
		–N(11)	2.21	–N(31)	2.22	
		–N(17)	2.20	–N(37)	2.22	
$Mo_2(OCH\text{-}t\text{-}Bu)_4(PMe_3)_4$ (5)	2.22	–P(3)	2.52	–P(11)	2.58	this work
		–P(7)	2.53	–P(15)	2.53	
		–O(19)	1.98	–O(31)	2.08	
		–O(25)	2.09	–O(37)	1.99	
$Mo_2(OC_6F_5)_4(HNMe_2)_4$	2.14	–O(2)	2.08			18a
		–O(4)	2.06			
		–N(1)	2.24			
		–N(3)	2.24			
$Mo_2(OC_6F_5)_4(PMe_3)_4$	2.15	–O(1)	2.14	–O(1)	2.06	18b
		–P(1)	2.64	–P(1)′	2.67	
		–O(2)	2.06	–O(2)	2.12	
		–P(2)	2.58	–P(2)′	2.61	

Specifically, we have studied the exchange of free *i*-PrOH with the bound *i*-PrOH in $Mo_2(O\text{-}i\text{-}Pr)_4(HO\text{-}i\text{-}Pr)_4$ (**1**). When compound **1** is dissolved in toluene-d_8 and *i*-PrOH is added, one sees the distinct signals associated with free *i*-PrOH and those of compound **1** at, and even above, room temperature. Thus intermolecular *i*-PrOH group exchange is slow on the NMR time scale, and this contrasts with the behavior of $Mo_2(O\text{-}i\text{-}Pr)_6$ dissolved in toluene-d_8, which shows rapid (NMR time scale) alkoxide/alcohol exchange (eq 6).

$$Mo_2(O\text{-}i\text{-}Pr)_6 + 6HO\text{-}i\text{-}Pr' \rightleftarrows Mo_2(O\text{-}i\text{-}Pr')_6 + 6HO\text{-}i\text{-}Pr \quad (6)$$

In eq 6, the isopropyl group labeled Pr′ is in fact equivalent to the unprimed group and the facile alcohol/alkoxide exchange presumably occurs by way of a rapid and reversible formation of $Mo_2(O\text{-}i\text{-}Pr)_6(HO\text{-}i\text{-}Pr)_2$, formulated as in **B**.

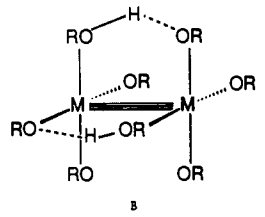

B

Although **B** has not been isolated, the related dimethylamine adduct $W_2(O\text{-}i\text{-}Pr)_6(HNMe_2)_2$ has been structurally characterized, showing that the N–H---O interactions across the W–W triple bond causes an eclipsed $W_2O_6N_2$ skeleton.[24] An alcoholate hydrogen atom transfer from alcohol to alkoxide followed by reversible elimination of alcohol could readily account for the lability of reaction **6**, which is only frozen out at *ca.* –80 °C on the NMR time scale.

It is thus apparent that compound **1** is less labile to *i*-PrOH exchange than the Mo–Mo triply bonded complex. In order to study the relative lability of the alcohol ligands in compound **1**, we carried out reactions in NMR tubes wherein **1** dissolved in toluene-d_8 was allowed to react with DO-*i*-Pr-d_7 (100 equiv). In these studies, the substitution of *i*-PrOH in **1** by DO-*i*-Pr-d_7 is indicated by the appearance of free protio-2-propanol. The exchange reaction was studied at –60, –50, and –40 °C and was

(24) Chetcuti, M. J.; Chisholm, M. H.; Huffman, J. C.; Leonelli, J. *J. Am. Chem. Soc.* **1983**, *105*, 292.

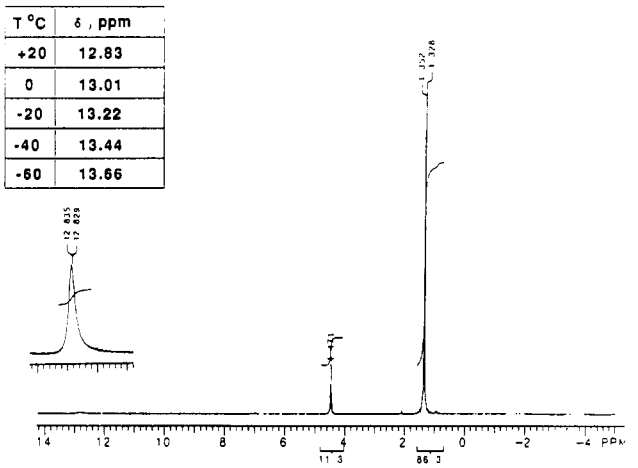

Figure 8. ^1H NMR variable-temperature studies of $Mo_2(O\text{-}i\text{-}Pr)_4(HO\text{-}i\text{-}Pr)_4$ (**1**).

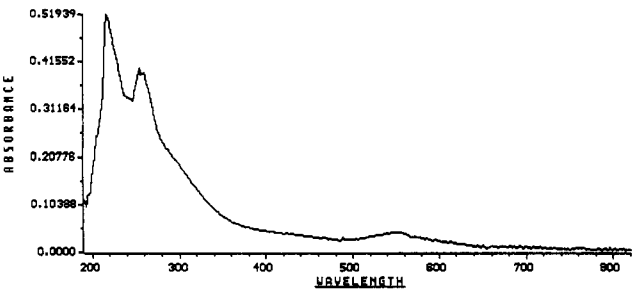

Figure 9. UV–visible spectrum of $Mo_2(O\text{-}i\text{-}Pr)_4(HO\text{-}i\text{-}Pr)_4$ (**1**).

monitored with time. As is shown in Figure 10, growth of free protio-2-propanol is quite slow. The relative concentrations of bound and free 2-propanol were estimated by integration, and the data were analyzed according to an irreversible pseudo-first-order kinetic scheme. With the use of a 100-fold excess of added DO-*i*-Pr-d_7, the liberation of protio-2-propanol is essentially irreversible. (We have in this study ignored the kinetic isotope effect arising from the presence of *i*-PrOD.) A plot of $\ln(k/T)$ *vs* $1/T$ yielded a straight line, and further analysis gave the activation parameters $\Delta H^* = 9.5(5)$ kcal mol^{-1} and $\Delta S^* = -34(3)$ eu.

While we have ignored the fact that *i*-PrOH/D dissolved in toluene-d_8 almost certainly exists as hydrogen-bonded dimers/trimers and may be even higher oligomers and we have not

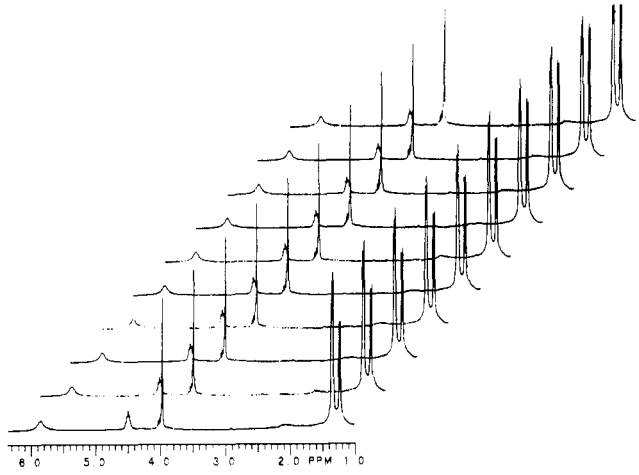

Figure 10. Exchange reaction of **1** with DO-*i*-Pr-d_7 at −50 °C monitored with time from $t = x + 0$ to $x + 26$ min. The solvent peaks are omitted for clarity. The singlet at 4.05 ppm is due to internal standard ferrocene.

considered the kinetic isotope effect that may arise from reactions employing *i*-PrOH vs *i*-PrOD, the above data do serve to indicate an associative mechanism for substitution.

Mo_2^{4+}-containing compounds may be considered as a general class of M_2^{4+} complexes of the formula $M_2(L_{eq})_8(L_{ax})_2$ as shown in **C**. These complexes are typified by M = Mo and M = Rh,

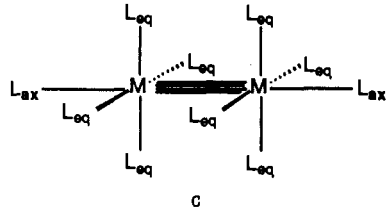

C

and the strength of the M–L bonding follows the order M–L_{eq} > M–L_{ax} and the rate of M–L_{ax} exchange is much greater than that for M–L_{eq}. This was shown for $[Rh_2(OAc)_2(MeCN)_4{\cdot}2MeCN]^{2+}$ [25] dissolved in CD_3CN as solvent which exchanges with the axial weakly bound MeCN ligands essentially instantaneously. On the other hand, the equatorial MeCN exchange with CD_3CN solvent was very slow ($t_{1/2}$ = *ca.* 4 h at 100 °C) and showed activation parameters $\Delta H^* = +33(1)$ kcal mol^{-1} and $\Delta S^* = +11(3)$ eu, consistent with bond breaking in the transition state.

Bowen and Taube[26] were the first to prepare the Mo_2^{4+}(aquo) ion which may reasonably be formulated as $[Mo_2(H_2O_{eq})_8(H_2O_{ax})_2]^{4+}$ though no structural information is known. Sykes and co-workers[27] investigated the substitutional behavior of Mo_2^{4+}(aquo) with respect to uptake of NCS^- and $HC_2O_4^-$. They noted an analogy with the substitution chemistry of d^0 and d^1 M≡O complexes, M = Ti and V, respectively, wherein rapid and reversible, essentially diffusion-controlled access to the axial position is possible. It is the slower and rate-determining access to the equatorial position that is of the relevance to our studies here and indeed to Sykes' measurements of the uptake of oxalate, $HC_2O_4^-$, and thiocyanate, NCS^-, ions.[27] In this regard, it is interesting to note that the activation parameters for $HC_2O_4^-$ uptake by the Mo_2^{4+}(aquo) ion are $\Delta H^* = 12.4(1)$ kcal mol^{-1} and $\Delta S^* = -23.2(2.6)$ eu and are very similar to those noted in our study of the alcohol exchange involving compound **1**. The substitution of alcohol in compound **1** may be compared with the substitution of carboxylate in the $Mo_2(O_2C\text{-}t\text{-}Bu)_5^-$ anion, which has recently been studied.[28] In the ground state, the anion has the structure depicted by **D**; however, in toluene-d_8 and CD_2Cl_2

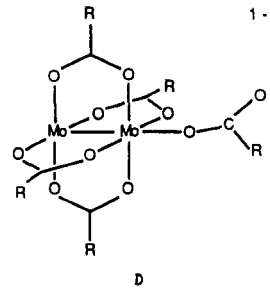

D

solution the $Mo_2(O_2C\text{-}t\text{-}Bu)_5^-$ anion displays fluxional behavior wherein the axial pivalate is exchanged with the μ-carboxylate groups. In compound **1** the presence of the hydrogen bonding in the ground-state structure makes the RO---HOR moiety essentially a chelating ligand spanning the Mo–Mo quadruple bond. In order for exchange with free alcohol to occur, this hydrogen bonding must be broken and a new hydrogen bond formed between an alkoxide ligand and the entering alcohol. We suggest that it is the availability of the low-lying Mo–Mo δ* orbital that facilitates this associative behavior in the substitution chemistry of the Mo_2^{4+} moiety. Pictorially this can be represented by E.

E

Concluding Remarks

The reaction shown in eq 2 leads to the formation of the substitutionally labile complex $Mo_2(O\text{-}i\text{-}Pr)_4(HO\text{-}i\text{-}Pr)_4$ (**1**), which appears to be a member of a series of complexes of formula $Mo_2(OR)_4(HOR)_4$. The compounds where R = *i*-Pr and c-Pen are hydrocarbon soluble and are sources of the Mo_2^{4+} moiety by simple alkoxide/alcohol substitution reactions. However, in some instances oxidative addition can be facile, leading to Mo_2^{6+}-containing compounds. This occurs, for example, in the reactions with certain sterically unencumbered olefins and is worthy of further investigation.[10a] Compounds of the formula $Mo_2(OR)_4L_4$ where L = a neutral donor ligand such as PMe_3 and py show anomalously long Mo–Mo quadruple bond distances as a result of filled–filled Mo d_π–O p_π interactions. Studies of the exchange of free 2-propanol-d_8 with **1** have provided a quantitative measure of the kinetic lability of compound **1** in a self-exchange reaction. Activation parameters $\Delta H^* = 9.5(5)$ kcal mol^{-1} and $\Delta S^* = -34(3)$ eu suggest that an associative mechanism is operative. These results compare favorably with the studies of Sykes and co-workers[27] on the substitutional behavior of the Mo_2^{4+}(aquo) ion. The similarity between compounds **1** and **2** and Mo_2^{4+}(aquo) is further emphasized by the assignment of the $\delta \rightarrow \delta^*$ transition at *ca.* 560 and 510 nm, respectively.

Experimental Section

Physical Techniques. ^1H NMR and ^{13}C NMR spectra were recorded on a Varian XL-300 or a Nicolet NT-360 spectrometer in dry and oxygen-free solvents. Infrared spectra were obtained from Nujol mulls between CsI plates or as hexane solutions (*vs* hexane) in KBr solution cells with the use of a Perkin-Elmer 283 spectrometer. Ultraviolet and visible absorption spectra were recorded on a Hewlett Packard 8452A diode array spectrophotometer using a 1.00-cm quartz cell. The spectra were recorded in dry oxygen-free tetrahydrofuran or hexane; from these was subtracted a spectrum of the neat solvent in the same cell.

Electrochemical measurements were obtained with a PAR 173 potentiostat and 175 programmer along with a Houston Instruments

(25) Casas, J. M.; Cayton, R. H.; Chisholm, M. H. *Inorg. Chem.* **1991**, *30*, 360.
(26) Bowen, A. R.; Taube, H. *Inorg. Chem.* **1974**, *13*, 2245.
(27) Finholt, J. E.; Leupin, P.; Sykes, A. G. *Inorg. Chem.* **1983**, *22*, 3315.
(28) Cayton, R. H.; Chacon, S. T.; Chisholm, M. H.; Folting, K. *Polyhedron* **1993**, *12*, 415.

2000 X-Y recorder. The cyclic voltamogram was recorded in an air-free cell under N_2 atmosphere in tetrahydrofuran, 2.0 M in tetra-*n*-butylammonium hexafluorophosphate as the supporting electrolyte. The working electrode was a glassy carbon electrode. The counter electrode was a platinum-gauze electrode. All potentials reported are relative to the $(C_5H_5)_2Fe/(C_5H_5)_2Fe^+$ couple.

Elemental analyses were performed by Alfred Bernhard Analytical Laboratories, and all compounds were handled with inert-atmosphere techniques.

Syntheses. Reactions were carried out using standard Schlenk techniques with dry, air-free solvents.

Mo_2(O-*i*-Pr)$_4$(HO-i-Pr)$_4$ (1). $Mo_2(i\text{-Bu})_2(NMe_2)_4$ (1.5 g, 3.1 mmol) was dissolved in hexane (5 mL). *i*-PrOH (20 mL) was added at 0 °C with stirring, which caused the solution to change color from yellow to deep purple in *ca.* 1 h. The solvent was removed under vacuum to yield a dark purple solid, which was redissolved in 5 mL of *i*-PrOH. A large mass of dark purple crystals formed upon cooling to −20 °C. ^{1}H NMR (toluene-d_8): δ 1.38 (d, 12H), 4.51 (sept, 2H), 13.10 (s, 1H). ^{13}C NMR (benzene-d_6): δ 27.30 (2), 67.27 (1). IR (hexane solution, cm^{-1}): 3280 (m, br), 1420 (s), 1358 (w), 1154 (m), 1110 (s), 1020 (w), 980 (s), 950 (s), 900 (m), 833 (s), 606 (m), 585 (m), 570 (m), 450 (m). Anal. Calcd for $C_{32}H_{60}Mo_2O_8$: C, 43.11; H, 9.05; N, 0.0. UV–vis data (8.9×10^{-5} M in hexane; extinction coefficient ϵ (M^{-1} cm^{-1}) in parentheses): 548 (473), 416 (466), 296 (2266), 256 (4336), 216 (5835).

Mo_2(O-c-C_5H_9)$_4$(HO-c-C_5H_9)$_4$ (2). $Mo_2(i\text{-Bu})_2(NMe_2)_4$ (0.15 g, 0.31 mmol) was dissolved in hexane (15 mL). c-C_5H_9OH (3 mL) was added at room temperature. The solution changed color from yellow to deep purple in *ca.* 1$^1/_2$ h. The solvent was removed under vacuum to yield a dark purple solid, which was redissolved in 5 mL of THF. Dark purple crystals formed upon cooling to −40 °C. ^{1}H NMR (benzene-d_6): δ 1.58 (br s, 4H), 1.72 (br m, 4H), 1.91 (br s, 8H), 4.77 (sept, 2H), 12.60 (s, 1H). IR (hexane solution, cm^{-1}): 3280 (m, br), 1420 (s), 1358 (w), 1154 (m), 1110 (s), 1020 (w), 980 (s), 950 (s), 900 (m), 833 (s), 606 (m), 585 (m), 570 (m), 450 (m).

Mo_2(OCH$_2$-*t*-Bu)$_4$(HNMe$_2$)$_4$ (3). $Mo_2(i\text{-Bu})_2(NMe_2)_4$ (1.0 g, 2.1 mmol) was dissolved in hexane (20 mL). A small amount of $HNMe_2$ was added from a calibrated gas line by vacuum transfer. Upon addition of *t*-BuCH$_2$OH (5.5 mL, 8.3 mmol), the solution changed from yellow to deep red-purple. After 45 min, the solvents were removed under vacuum to give a dark purple solid, which was recrystallized from hexane (3 mL) to produce $Mo_2(OCH_2\text{-}t\text{-Bu}))_4HNMe_2)_4$ in 65% yield. ^{1}H NMR (toluene-d_6, 20 °C): δ 1.05 (s, 9H), 3.51 (s, 2H), 2.64 (d, 6H), 7.08 (sept, 1H). ^{13}C NMR (benzene-d_6): 27.52 (3), 34.72 (1), 42.27 (2), 76.65 (1). IR (hexane solution, cm^{-1}): 3209 (m, br), 2680 (m), 1600 (m, br), 1360 (s), 1290 (m), 1260 (w), 1220 (m), 1128 (m), 1080 (vs), 1020 (vs), 932 (m), 910 (s), 758 (m), 660 (s), 640 (s), 472 (m), 400 (m). Anal. Calcd for $C_{28}H_{72}Mo_2N_4O_4$: C, 46.66; H, 10.07; N, 7.77. Found: C, 46.46; H, 9.90; N, 7.60. UV–vis data (2.8×10^{-3} M in hexane; extinction coefficient ϵ (M^{-1} cm^{-1}) in parentheses): 585 (1200), 280 (7400).

Mo_2(O-*i*-Pr)$_4$(py)$_4$ (4). *i*-PrOH (10 mL) was added to the solution of $Mo_2(i\text{-Bu})_2(NMe_2)_4$ (1.19 g, 2.47 mmol) in hexane. The solution turned dark blue-purple and was evacuated to dryness after 30 min. The purple solid was redissolved in hexane (5 mL), and pyridine (0.8 mL, 9.9 mmol) was added, which caused the solution to turn dark brown. Dark brown crystals of Mo_2(O-*i*-Pr)$_4$(py)$_4$ formed upon cooling to −20 °C. ^{1}H NMR (toluene-d_8): 1.48 (d, 6H), 5.59 (sept, 1H), 6.68 (t, 1H), 7.00 (dd, 2H), 8.48 (d, 2H). IR (Nujol, cm^{-1}): 1600 (w), 1450 (m), 1350 (2), 1315 (w), 1260 (w), 1212 (w), 1155 (m), 1118 (s), 976 (s), 962 (m), 951 (m), 830 (m), 760 (w), 700 (m), 690 (m), 587 (s), 575 (m), 468 (w), 420 (w). Anal. Calcd for $C_{36}H_{48}Mo_2N_4O_4$: C, 51.62; H, 6.50; N, 7.52. Found: C, 51.34; H, 6.53; N, 7.40. UV–vis data (THF solution, 6.7×10^{-5} M; extinction coefficient ϵ (M^{-1} cm^{-1}) in parentheses): 334 (2495), 254 (8956), 218 (14104).

Mo_2(OCH$_2$-*t*-Bu)$_4$(PMe$_3$)$_4$ (5). $Mo_2(OCH_2\text{-}t\text{-Bu})_4(HNMe_2)_4$ (0.45 g, 0.62 mmol) was dissolved in hexane (5 mL), and the solution was frozen at −196 °C. PMe_3 (3.1 mmol, 5 equiv) was added from a calibrated gas line by vacuum transfer. Upon warming, the solution was allowed to stir for 1 h at room temperature. Emerald green crystals of $Mo_2(OCH_2\text{-}t\text{-Bu})_2(PMe_3)_4$ formed when the solution was cooled to −20 °C. ^{1}H NMR (toluene-d_8): δ 1.08 (s, 9H), 3.95 (s, 2H), 1.56 (br s, 9H). IR (Nujol, cm^{-1}): 1383 (m), 1365 (m), 1358 (s), 1290 (m), 1270 (m), 1210 (w), 1147 (w, br), 1108 (s), 1060 (s), 1040 (m), 1015 (s), 947 (s), 890 (w), 847 (m), 800 (w, br), 752 (m), 720 (s), 644 (s), 596 (s), 444 (w, br), 407 (w). Anal. Calcd for $C_{32}H_{80}Mo_2O_4P_4$: C, 45.50; H, 9.55; N, 0.0. Found: C, 45.32; H, 9.46; N, <0.05. UV–vis data (2.4×10^{-3} M in hexane; extinction coefficient ϵ (M^{-1} cm^{-1}) in parentheses): 696 (900), 484 (930), 406 (1800).

Crystallographic Studies. General procedures and listings of programs have been previously given.[29] A summary of crystal data is given in Table I. Listings of atomic coordinates for compounds **1–5** are given in Tables II–VI. For the sake of brevity, the specific comments on the solution of each structure have been removed to the supplementary materials, where complete crystallographic data are available.

Acknowledgment. We thank the National Science Foundation for financial support and Dr. Theodore Budzichowski for assistance in the evaluation of the kinetic data.

Supplementary Material Available: For **1–5**, a textual summary of structural solutions, tables of complete bond distances and angles and anisotropic thermal parameters, and VERSORT drawings and stereoviews with atom-numbering schemes (33 pages). Ordering information is given on any current masthead page.

(29) Chisholm, M. H.; Folting, K.; Huffman, J. C.; Kirkpatrick, C. C. *Inorg. Chem.* **1984**, *23*, 1021.